AN AGCM +SSiB MODEL SIMULATION ON CHANGES IN PALAEOMONSOON CLIMATE AT 21 KA BP IN CHINA*

CHEN Xing (陈 星),

Department of Atmospheric Sciences, Nanjing University, Nanjing 210093

YU Ge (于 革) and *LIU Jian* (刘 健)

Nanjing Institute of Geography and Limnology, Chinese Academy of Sciences, Nanjing 210008

Received February 15, 2000; revised November 15, 2000

ABSTRACT

The numerical simulation experiment of climate at Last Glacial Maximum (LGM, 21 ka BP) in China is made by using an atmospheric general circulation model (AGCM) coupled with land surface processes (AGCM+SSiB) and earth orbital parameters and boundary forcing conditions at 21 ka. The modeled climate features are compared with reconstructed conditions at 21 ka from paleo-lake data and pollen data. The results show that the simulated climate conditions at 21 ka in China are fairly comparable with paleo-climatological data. The climate features at 21 ka in China from the experiment are characterized by a drier in the east and a wetter in the west and in the Tibetan Plateau as well. According to the analysis of distribution of pressure and precipitation, as well as the intensity of atmospheric circulation at 21 ka, monsoon circulation in eastern Asia was significantly weak comparing with the present. In the Tibetan Plateau, the intensity of summer monsoon circulation was strengthened, and winter monsoon was a little stronger than the present. The simulation with given forcing boundary conditions, especially the different vegetation coverage, can reproduce the climate condition at the LGM in China, and therefore provides dynamical mechanisms on the climate changes at 21 ka.

Key words: Last Glacial Maximum (LGM), climate modeling, Tibetan Plateau, monsoon

I. INTRODUCTION

The Last Glacial Maximum (21 ka BP) nowadays is a hot topic in the field of paleoclimate study. Recently, a lot of researched results from data analysis of palaeoclimate and numerical simulation have revealed that global climate at 21 ka is very different from the present for the existence of Northern-Hemispheric ice sheets, low concentration of CO_2, different sea surface temperatures (SSTs), and orbital-forcing insolation anomalies (CLIMAP Members 1981; COHMAP Members 1988; Harrison et al. 1996; Kotlia et al. 1997; Street-Perrott et al. 1989; Tarasov et al. 1994; Tarasov et al.

* Supported by "Hundred Talents Project" from Chinese Academy of Sciences (CAS 1998-0019) and from the National Natural Science Foundation of China (49971075), and "Creative Project" from Lake Sediment and Environment Laboratory (C200289).

1999; Wright et al. 1993; Yu and Harrison 1995). Quaternary researches in China reveal very different climate patterns at 21 ka comparing with the present in China. They are unique and special in the world (Chen et al. 1990; Li et al. 1988; Li et al. 1994; Li et al. 1995; Liew et al. 1998; Qin and Yu 1998; Shen and Xu 1994; Sun et al. 1995; Wang et al. 1990; Yan et al. 1998; Yao et al. 1994). The palaeoclimate at 21 ka in China has been reconstructed and the results indicated that there were very different dry and wet climate patterns in the east and the west, and a dramatical decrease in temperature appeared in this area. But it has not been understood the dynamical mechanism and atmospheric circulation background of the climate anomalies. Some numerical experiments have been conducted just for the global climate at 21 ka (Dong et al. 1996; Joussaume and Taylor 1995; Kutzbach et al. 1998). But so far no good simulation results of paleoclimate experiments have been reported about the climate change in China at the LGM, especially the explanations of mechanism of East Asian monsoon variations.

In this study, based on the analysis of different sources of paleo-climatological records, by using a general atmospheric circulation model (AGCM) coupled with a simplified land process model (SSiB) (e. g. AGCM + SSiB) and boundary conditions, climate conditions at 21 ka in China are reproduced and the possible dynamical mechanisms are explored. By comparing reconstructed climate from various proxy indices with atmospheric circulation features from the model, the major characteristics associated with the potential mechanisms of climate change at 21 ka in China are addressed preliminarily.

II. MODEL AND FORCING CONDITIONS

1. *Climate Model and Experiment Design*

The model used in this study is a general atmospheric circulation model, coupled with the land surface processes (AGCM+SSiB). This AGCM is an improved version of 9 levels spectral model truncated at wave number 15 (Liu and Wu 1995; 1997; Wu et al. 1996). The spatial resolution in horizontal directions is about 7. 5°×4. 5°. SSiB is a simplified biosphere model (Sellers et al. 1986; Xue et al. 1991). In this model, there are one vegetation layer and three soil layers, in which vegetation is classified into eleven types. In our experiment, the output of SSiB is incorporated with AGCM.

The experiment is designed according to Paleo-climate Modeling Inter-comparison Project (PMIP). It is used to determine the model predicted equilibrium climate that is consistent with certain imposed changes in boundary condition characteristics of the period under study. Here, the boundary conditions indicate the various prescribed conditions, including orbital parameters which determine the insolation pattern, atmospheric CO_2, glacial ice distribution and sea surface temperatures. These conditions are considered to be external to the components of the climate system considered by typical GCMs. By considering equilibrium climate states, the study limits the kinds of issues that can be addressed concerning the evolution of climate from the state to another. For the LGM, two experiments are designed in PMIP. In one experiment, SSTs are prescribed, while in the other experiment, they are created by model. In this study, the first method is used and the massive ice sheets covering North America and Scandinavia have been prescribed

according to reconstruction by Peltier (1994). It is very important that the LGM climate is characterized by large changes in the surface boundary conditions (ice sheet extent and elevation, SST, and surface albedo) and atmospheric carbon dioxide concentration, but only minor changes in the insolation pattern (Berger 1988). This period (21 ka BP) is very important for understanding how ice sheets and lowered CO_2 levels influence climate. Among the climate features of interest in this experiment are only the simulated changes in the Northern Hemisphere jet stream location and associated changes in the storm tracks (Gates 1976; Valdes and Hall 1994; Manabe and Broccoli 1985; Rind 1987; Kutzbach and Guetter 1986; Joussamue 1993). As our knowledge, there is no numerical simulation study focus on Asian monsoon climate features in China at 21 ka. Therefore, in this study, we design the experiment and attempt to simulate the climate at 21 ka in East Asia and China.

2. 21 *ka Simulation*

In this experiment, the 21 ka simulation is driven by two kinds of forcing conditions. One is associated with solar radiation, e. g. earth orbital parameters (perihelion, eccentricity and obliquity). The other is associated with the earth surface conditions, including SST, snow and ice coverage, atmospheric CO_2 concentration and vegetation. In order to identify the climate change at 21 ka from the present, we run both 0 ka and 21 ka experiments. In the 0 ka (control) test, SST is the present data with 10-year variation. Snow and sea ice coverage are with seasonal variation, vegetation distribution and earth orbital parameters are same as the present. CO_2 concentration is 280 ppm. In the 21 ka experiment, SSTs, sea ice, snow cover and ice sheet are determined based on PMIP document. CO_2 concentration is 200 ppm, and earth orbital parameters are estimated according to Berger's work (1978). Some researches indicated that interaction between vegetation and atmosphere is very important in climate simulation (Foley et al. 1994; Martin et al. 1999; Winkler and Wang 1993; Wang 1999). In this study, vegetation distributions at 21 ka in East Asia are prescribed according to pollen data (Yu et al. 1999). All forcing conditions are summarized in Table 1. For both 21 ka and control experiments, 11 modeling year simulation was run, and averages of the last 10 years were treated as mean equilibrium climate conditions. Here, 10-year average is used as a typical period of climate status at 21 ka to be compared with the present climate.

Table 1. The Earth Orbital Parameters and Boundary Conditions for Simulation Experiments

Parameters	The earth orbital parameters			Boundary conditions
	Eccentricity	Perihelion	Obliquity	
Present (0 ka)	0.0167	282.04	23.446	280 ppm CO_2 concentration, 10-year SST, present snow and sea ice cover, present vegetation distribution
21 ka BP	0.0187	294.42	22.949	200 ppm CO_2 concentration, SST from CLIMAP, snow and ice sheet from PMIP, vegetation distribution changed over Eurasia from geological data

3. *Model Validation*

The modeled results are validated by comparison between control experiment and observed data. The sea level pressure, temperature, geopotential height at 500 hPa from model output are consistent very well with NCEP/NCAR data (Liu et al. 1999, PIMP Workshop III). The main features of precipitation distribution are generally good, and only in some regions from tropical zone show a little deviation from NCEP/NCAR data. Overall, the model used in this paper has good capability for climate simulation, especially in the area of China.

III. RESULTS

1. *Modeled Climate Features at 21 ka in China*

The simulated surface temperature, precipitation and effective precipitation P−E at 21 ka in the area of China are shown in Fig. 1. The annual mean surface temperatures, shown in Fig. 1a are from 20°C to −20°C with the region from Hainan Island, southern China, to northeastern China. Annual mean surface temperature in the Tibetan Plateau is about −5°C to −10°C, the one of the coldest regions by the model simulation, and the another one is northeastern China. It can be seen from Fig. 1b that there is a high annual precipitation in the Tibetan Plateau region. The maximum precipitation is more than 2.5 mm/d, the most of the Plateau is covered by areas of 1.5 mm/d. There is the region covered by 2.5 mm/d in the north of China. On the contrary, precipitation in eastern and southeastern China is less than 2.5 mm/d. Indices representing dry and wet conditions (annual effective precipitation P − E) are mapped in Fig. 1c. The pattern of P − E distribution is very similar to that of precipitation. The maximum is in the Tibetan Plateau. In the middle and south of the Plateau, P−E is greater than 1.5 mm/d, and the maximum is about 2 mm/d. As a contrast, P − E is less than 1 mm/d in the eastern China, which is much less than that in the Plateau. This distribution shows that there was humid climate in the Tibetan Plateau and drier climate in the east of China at 21 ka.

From above results we can find the main climate features at 21 ka in China, i.e. it is colder and wetter in the Tibetan Plateau and warmer and drier in eastern China compared with the Plateau. The differences of the climate between 21 ka and the present are shown in Fig. 2. From the differences of annual mean temperature (Fig. 2a), it can be seen that decreases in temperature ranged between 1°C to 10°C at 21 ka. In the plateau, temperature decreasing in summer is less than that in winter. This indicates that climate was warmer in summer half year in the Tibetan Plateau. The anomalies of annual precipitation at 21 ka (Fig. 2b) show that the positive anomalies are located at the Tibetan Plateau, northwest of Xinjiang, north and northeast of China. The differences of annual precipitation are negative in the regions where precipitation is plentiful at present, such as the east and the southeast of China. Especially in the upper and middle basins of Yangtze River, the decrease in precipitation is more than 1 mm/d. It means that these areas are short of precipitation at 21 ka. The distributions of difference of annual effective precipitation (P−E) are almost the same as that of annual precipitation (Fig. 2c).

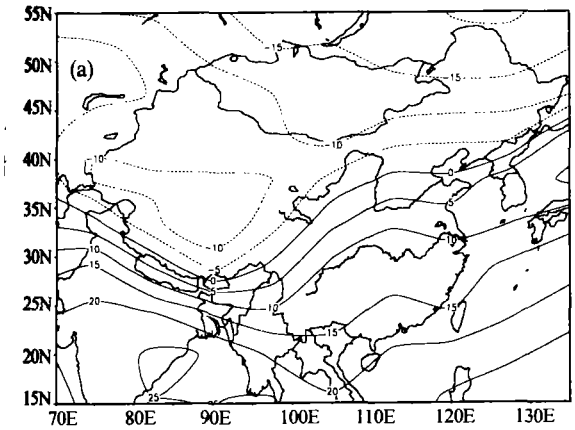

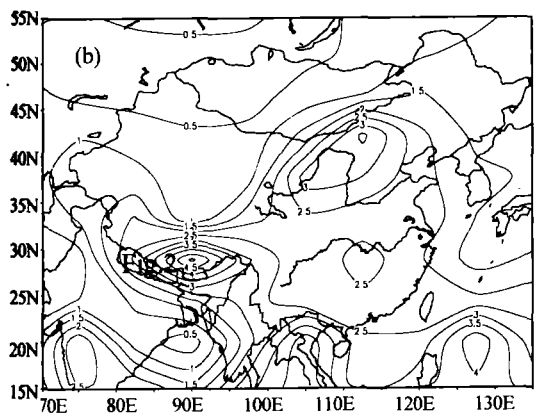

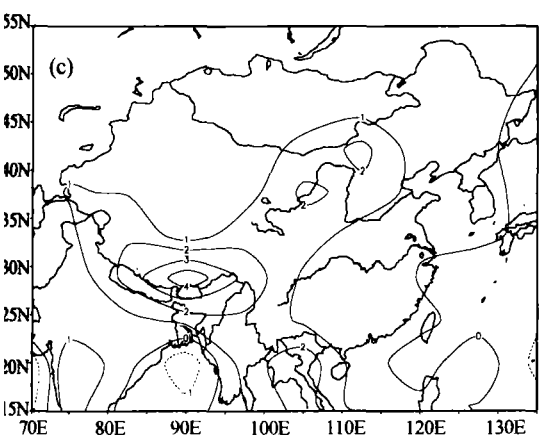

Fig. 1. Simulated the 21 ka BP annual mean temperature (℃) (a), annual mean precipitation (mm/d) (b) and annual mean effective precipitation (mm/d) (c).

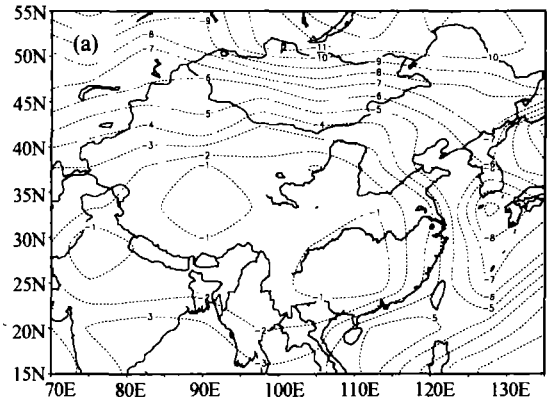

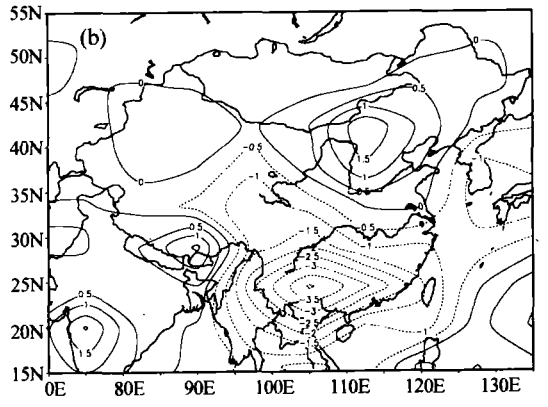

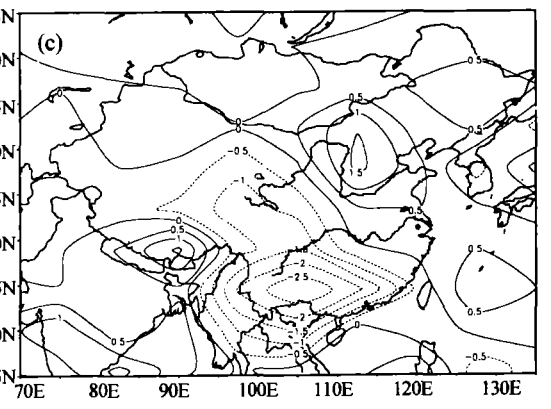

Fig. 2. Simulated differences between 21 ka BP and 0 ka of annual mean temperature (℃) (a), annual mean precipitation (mm/d) (b) and annual mean effective precipitation (mm/d) (c).

From the simulation of 21 ka conditions, we can find that it is colder in China at 21 ka than the present, and the spatial patterns of humidity conditions are almost inverse between 21 ka and present, e. g., it is wetter in the west and drier in the east of China at 21 ka.

2. *Comparison between the Simulation and Paleoclimate Evidence of* 21 *ka*

The simulation of climate at 21 ka is validated by using various palaeoclimate evidence. In this subsection, reconstructed lake status and vegetation pattern at 21 ka in China from paleo-lake-status database and pollen database (Fig. 3), which can be used as indices of the climate conditions, are compared with the model simulation results.

It can be seen from Fig. 3a that lake-water levels are lower at present in the northwest, north and northeast of China, and they are higher in southern and southeastern China today. The conditions registered by lake-status are basically matched the precipitation distribution in the present China. The data of 21 ka (Fig. 3b) show high lake water levels in the Tibetan Plateau and northwestern China and the low levels in the eastern China. These reconstructed climate features at 21 ka were wet in the west and dry in the east of China. The distribution of vegetation patterns in Figs. 3c and 3d shows cold and humid conditions in the northeast of China. As a comparison, modern vegetation patterns in the southeast of China is indicating warm and wet condition, the steppe and desert vegetation respond to arid condition in the northeast and northwest of China, while the tundra in eastern Tibetan Plateau is controlled by alpine cold and wet conditions. In these regions climate is colder and drier. While at 21 ka in China, the vegetation in the most eastern China, except for the coastal zone of southeast, was characterized by the steppe and deserts. There were some vegetations fit to humid climate in the Tibetan Plateau and the northeast of China. Therefore the climate in these regions was cold and humid, and consistent with the distributions of modeled precipitation and effective precipitation shown as Fig. 2.

IV. THE 21 KA CLIMATE DIAGNOSES

Based on the basic atmospheric circulation fields of the simulation at 21 ka, and analogue to modern climate, we attempt to understand the mechanisms and causes of climate at 21 ka and their changes from the present in China.

1. *Sea Level Pressure*

The simulated sea level pressure of 21 ka and 0 ka and their differences in summer and winter in eastern Asia and western Pacific are shown in Fig. 4. It shows that sea level pressure in the western Pacific in summer at 21 ka is lower than that at present, so that the differences are negative. Over eastern Asia Continent the pressure differences in summer are positive in most part of China. This means that the India low-pressure system that controlled continent in summer was weaker at 21 ka than that today. Therefore, the sea level pressure differences between sea and land at 21 ka are smaller than the present, and lead to the weakened summer monsoon system over the Pacific. As a consequence of that, precipitation in eastern China decreased significantly and climate turned to drier at 21

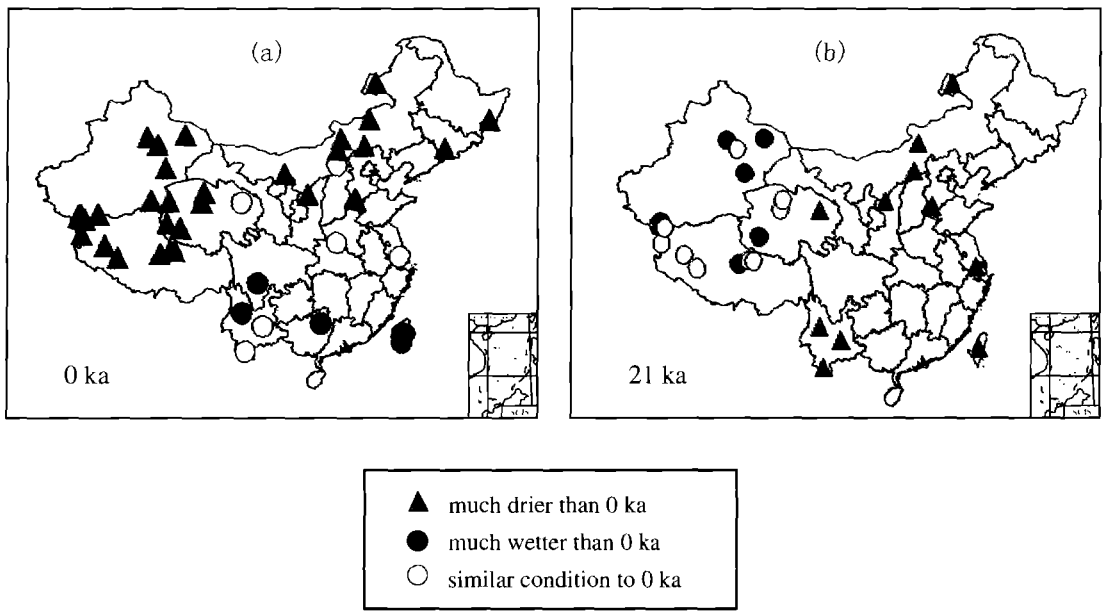

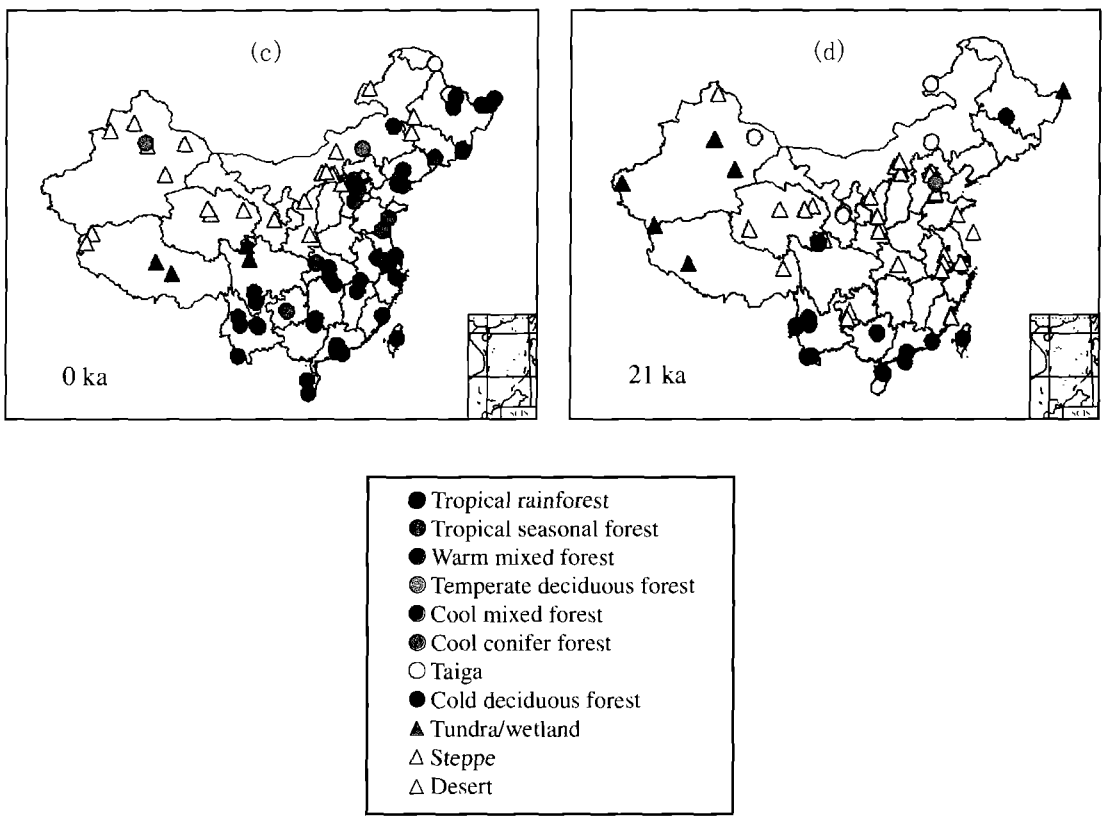

Fig. 3. Lake (a), (b) and pollen (c), (d) based reconstructions at the 21 ka and 0 ka BP.

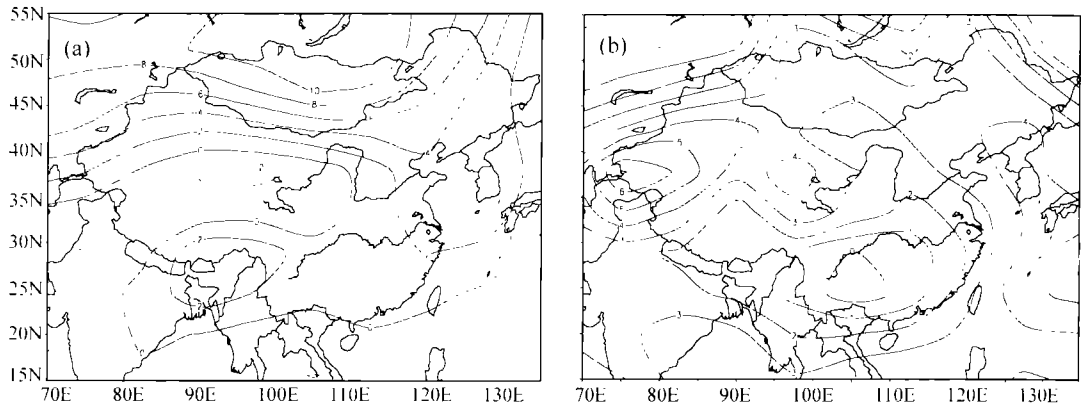

Fig. 4. Differences of sea level pressure from 21 ka to 0 ka in summer (a) and winter (b).

ka. On the other hand, the low pressure system in the west of China was strengthened and precipitation increased, and climate became humid at 21 ka in summer. In winter, the differences of sea level pressure distribution features are that Mongolia high and Aleutian low were strengthened and climate was much colder and less precipitation for the strong winter monsoon system and cold air mass extended southward.

2. *Streamlines*

Streamlines at 700 hPa in summer and winter at 21 ka and 0 ka are given in Fig. 5. The distribution of streamlines in summer at 0 ka shows that main anticyclonic circulation system is in western Pacific. As a result, the east of China is controlled by warm and moist air flow from the Bay of Bengal and South China Sea and there is a closed convergent center in the east of Tibetan Plateau. This streamline distribution pattern is important because in the summer a great deal of humid and warm air enters and converges in this area. For the present in China, water vapor in summer is from the south. Meanwhile the northwestern China is controlled by anticyclonic circulation and thus there is less precipitation in summer.

The simulated summer streamline distribution at 21 ka indicated some different features from 0 ka as shown in Fig. 5b. The features of streamlines at 21 ka are: (1) There was a convergent center in the Tibet in summer and it enabled the water vapor from South China Sea entering into and converged in Tibetan Plateau, northern and northwestern China. As a result of that the climate in these regions became more humid in summer. (2) Anticyclonic system of northwestern Pacific was more westward into the Asia inland and led to a dry climate in summer in the east of China. (3) In the north of China, the parts of Hebei and Inner Mongolia are another convergent area, here warm and moist air was joint with cold air of westerlies and formed precipitation. The distribution of these convergent areas is good consistent with the distribution of precipitation at 21 ka simulation.

3. *Monsoon Index*

Climate in eastern Asia is associated with the eastern Asia monsoon circulation

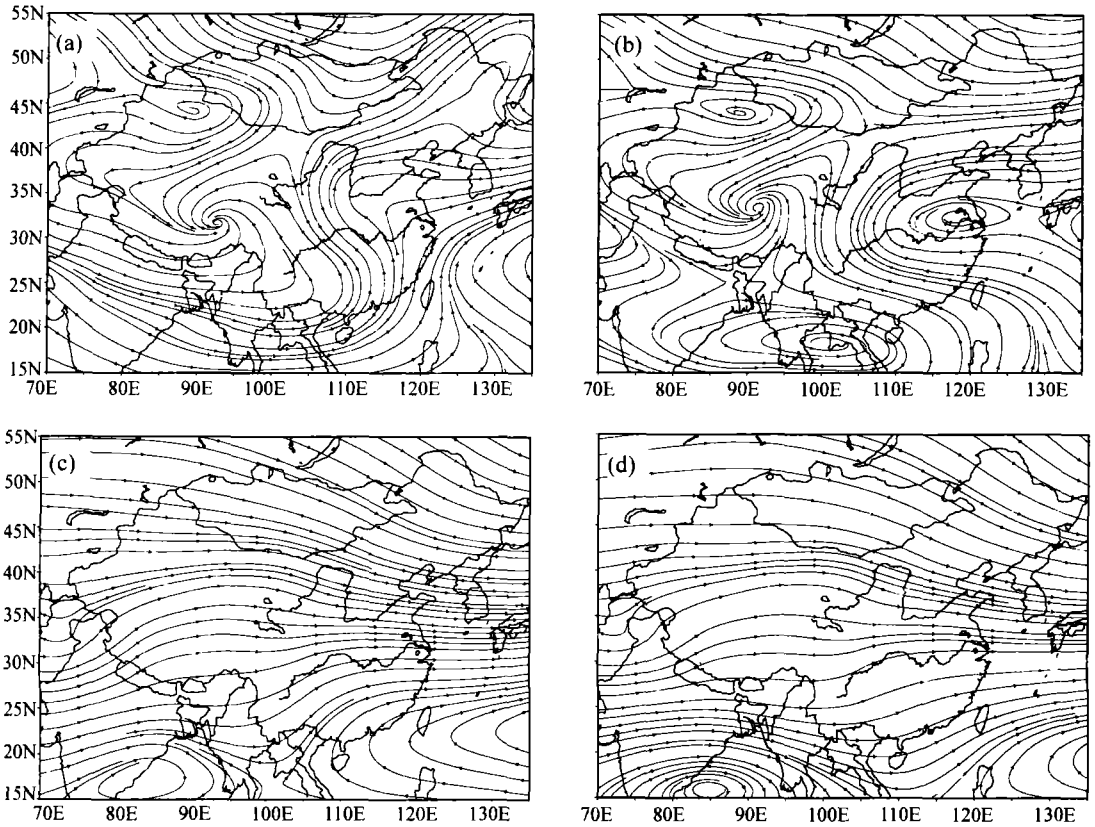

Fig. 5. Simulated 700 hPa streamline in summer (a), (b) and winter (c), (d) at 21 ka and 0 ka.

intensity and extent. The factors, controlling the intensity and extent of the eastern Asia monsoon, are complicated. The major factors that we pay more attentions to are sea level pressure differences between sea and land, dynamics of large topography such as Tibetan Plateau, and shift of planetary systems. In order to study how these three factors affect the climate changes at 21 ka, two monsoon indices are defined to indicate differences between sea and land and topography dynamical roles of Tibetan Plateau. Then wind vector fields at 1000 hPa are compared for determining the shift of planetary wind systems.

The index of sea-land sea level pressure differences is defined as

$$\Delta P_{sl} = \Delta P_{21} - \Delta P_0, \tag{1}$$

where ΔP_{21} andΔ P_0 are sea level pressure differences between land and sea (land minus sea) at 21 ka and 0 ka, respectively. The sea level pressure over finite topography has been reduced from surface pressure assuming hydrostatic balance and a lapse rate of $-6.5°$ km^{-1} (McAvaney et al. 1978). Therefore, ΔP_{sl} is the difference between 21 ka and 0 ka, indicating the change of the pressure differences from 21 ka to 0ka. The areas for ΔP_{sl} calculation are the windows of 80—120°E and 20—50°N (land) and 120—170°E and 20—50°N (sea). The index for Tibetan Plateau dynamical role is defined as

$$\Delta P_{tp} = \Delta P_{21}^{*} - \Delta P_0^{*}, \tag{2}$$

where ΔP_{21}^{*} and ΔP_{0}^{*} are sea level pressure differences between the plateau and low land (plateau minus low land) at 21 ka and 0 ka, respectively. Here, ΔP_{tp} represents pressure difference change from 21 ka to 0 ka. The window for Tibetan Plateau is 80—100°E and 30—40°N and for low land it is 80—120°E and 20—50°N (the plateau area is removed from this area when calculating the pressure differences).

From the above definition of two indices we can know that when $\Delta P_{sl}>0$ then it indicates that pressure differences between sea and land at 21 ka are greater than that at present and monsoon circulation became stronger, and vice versa, if $\Delta P_{sl}<0$, the monsoon became weaker at 21 ka. If $\Delta P_{p}>0$ then the plateau monsoon at 21 ka became stronger than today and it became weaker when $\Delta P_{tp}<0$. All parameters in Eqs. (1) and (2) are calculated for summer and winter at 21 ka and 0 ka (Table 2). The indices in Table 2 show that in winter both ΔP_{sl} and ΔP_{tp} are small, indicating that monsoon circulation driven by sea-land differences and large topography does not significantly change at 21 ka. However, the change in intensity of summer monsoon at 21 ka is significant compared with winter monsoon. As the decrease in pressure between sea and land, the summer monsoon at 21 ka became weaker than today, ΔP_{sl} is −3.42 hPa. On the other hand, ΔP_{tp} is 2.57 hPa, showing Tibetan Plateau summer monsoon at 21 ka stronger than 0 ka due to the topographical dynamics. This is the potential cause leading to more precipitation and humid climate in the plateau. In addition, the change of wind vector fields controlled by seasonal shifting of planetary wind systems (Figs. 6a and 6b) is an important factor for monsoon system in eastern China. Wind vectors show that the change of wind directions at 1000 hPa from summer to winter at 21 ka is not significant in southeastern China. It means there were no significant seasonal changes of surface wind directions in southeastern China and no strong summer monsoon presented at 21 ka. In summary, the modeled eastern Asia summer monsoon circulation at 21 ka is weaker than today in the southeast of China, and the Tibetan Plateau summer monsoon became stronger at 21 ka than the present.

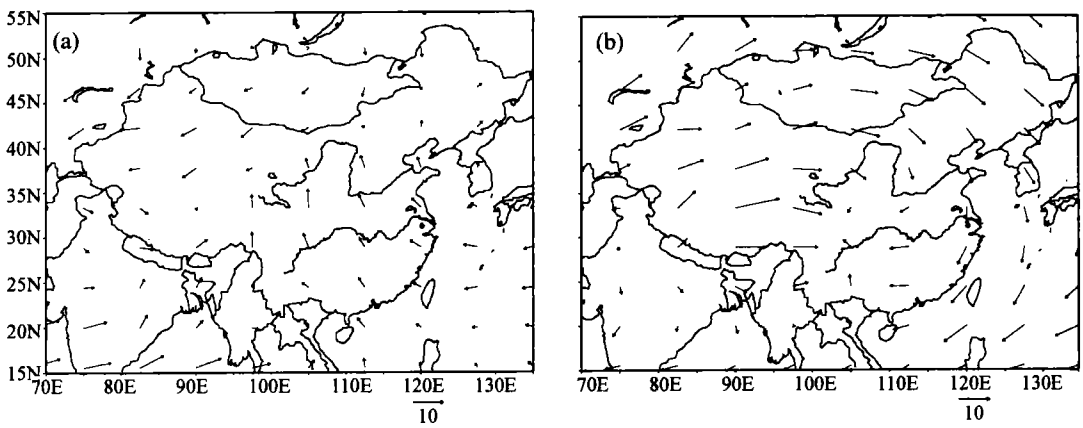

Fig. 6. Simulated 1000 hPa wind fields in summer (a) and winter (b) at 21 ka and 0 ka.

Table 2. Pressure Index Indicating Change of Monsoon Intensity

	Winter			Summer		
	21 ka	0 ka	21 ka−0 ka	21 ka	0 ka	21 ka−0 ka
Pressure difference between land and sea	8.20	7.59	0.61	11.46	14.88	−3.42
Pressure difference between low land and Tibet	9.34	9.38	−0.04	12.95	10.38	2.57

V. DISCUSSION AND CONCLUSION

The preliminary simulation results of climate at 21 ka in China discussed above give the typical climate conditions that have been addressed by a lot of geological data. This is the first effort on using AGCM+SSiB model to explore climate at 21 ka in China and it is fairly consistent with reconstructed paleoclimate. Before then there were some simulation experiments by using CCMs and UGAMP, but these experiments could not give realistic East Asia monsoon system signal and precipitation field. In our study, modeled East Asia monsoon system is better and 21 ka simulation is agreed with geological evidences.

Based on the comparison between model output and data analysis, we can draw the following conclusions:

(1) The modeled results of AGCM + SSiB with 21 ka boundary conditions and changed vegetation distribution experiment predicted the completed different conditions at 21 ka from the present in China, i.e. dry conditions in the eastern China and humid conditions in the Tibetan Plateau. This result is consistent with paleoclimate evidence and shows the different climate at 21 ka compared with the present. This is the first successful simulation that captured the climate features in China at 21 ka.

(2) Decreases in temperature at 21 ka in China are significant. The range of temperature decrease is from 1 ℃ to 10℃.

(3) The changes of eastern Asia monsoon circulation are dramastically in summer at 21 ka. The weaker summer monsoon is associated with the decreasing in pressure differences between land and sea, while in the Tibetan Plateau the summer monsoon is strengthened.

Many thanks are extended to Prof. SHI Yafeng, Prof. QIAN Yongfu, Prof. WANG Sumin and ZHANG Qiong, SHAO Hui, REN Xuejuan, for their kind help.

REFERENCES

Berger, A. (1978), Long-term variations of daily insolation and quaternary climatic changes, *J. Atmos. Sci.*, **35**: 2362−2367.

Berger, A. (1988), Milankovitch theory and climate, *Reviews of Geographics*, **26**: 624−657.

Chen Kezao, Bower, J. and Kelts, K. (1990), Changes in climate on Qinghai-Xizang plateau during the last 40000 years, *Quaternary Sciences*, (**1**): 21−30.

CLIMAP Members (1981), Seasonal reconstructions of the earth's surface at the Last Glacial Maximum, Geological Society of America Map Chart Series 36.

COHMAP Members (1988). Climatic changes of the last 18000 years: Observations and model simulations. *Science*, **241**: 1043—1052.

Dong Buwen, Valdes, P. and Hall, N. (1996). The changes of monsoonal climates due to earth's orbital perturbations and ice age boundary conditions. *Palaeoclimates*, **1**: 203—240.

Foley, J., Kutzbach, J. E., Coe, M. T. et al. (1994). Feedbacks between climate and boreal forests during the Holocene epoch. *Nature*, **371**: 52—54.

Gates, W. L (1976). The numerical simulation of ice-age climate with a global general circulation model. *J. Atmos. Sci.*, **33**: 1844—1873.

Harrison, S. P., Yu, G. and Tarasov, P. (1996). Late quaternary lake-level records from northern Eurasia. *Quaternary Research*, **45**: 138—159.

Joussaume, S. and Taylor, K. E. (1995). Status of the Paleoclimate Modeling Intercomparison Project (PMIP). In: Proceedings of the First International AMIP Scientific Conference (Monterey, California, USA, 15—19 May 1995). *WCRP Report*, **92**: 425—430.

Joussaume, S. (1993). Paleoclimatic tracers: An investigation using an atmospheric general circulation model under ice age conditions, Part 1: desert dust. *J. Geophys. Res.*, **98**: 2767—2805.

Kotlia, B. S., Bhalla, M. S., Sharma, C. et al. (1997). Palaeoclimatic conditions in the upper Pleistocene and Holocene Bhimtal-Naukuchiatal lake basin in south-central Kumaum, *North India*, *Palaeogeography, Palaeoclimatology, Palaeoecology*, **130**: 307—322.

Kutzbach, J. E., Gallimore, R., Harrison, S. P. et al. (1998). Climate and biome simulation for the past 21,000 years. *Quaternary Science Reviews*, **17**: 473—506.

Kutzbach, J. E., and Guetter, P. J. (1986). The influence of changing orbital parameters and surface boundary conditions on climate simulation for the past 18,000 years. *J. Atmos. Sci.*, **43**: 1726—1759.

Li Bingxiao., Cai Biqin and Liang Qingsheng (1988). Sedimentary characteristics of Aiding Lake, Tulufan Basin. *Chinese Science Bulletin*, **33**: 608—610.

Li Bingyuan, Li Yuanfang, Kong Zhaochen et al. (1994). Environmental changes during last 20 ka in the Gounongcuo Regions, Kekexili, Tibet. *Chinese Science Bulletin*, **39**: 1727—1728.

Li Yuanfang, Zhang Qingsong and Li Bingyuan (1995). Ostracode and its environmental evolution during late Pleistocene in the west Tibet. In: Committee of Tibet Research of China (Editor). *Collections Paper for Meeting of Tibetan Plateau and Global Changes*. China Meteor. Press, Beijing. pp. 52—61 (in Chinese).

Liew, P., Kuo C., Huang, S. et al. (1998). Vegetation change and terrestrial carbon storage in eastern Asia during the Last Glacial Maximum as indicated by a new pollen record from central Taiwan. *Global and Planetary Change*, pp. 16—17; pp. 85—95.

Liu, Hui, and Wu Guoxiong (1995). Description for a 9-layer Spectral Climate Model (L9R15). LASG Technical Report No. 3.

Liu Hui and Wu Guoxiong (1997). Impacts of land surface on climate of July and onset of summer monsoon: a study with an AGCM plus SSiB. *Adv. Atmos. Sci.*, **14**: 290—308.

Liu Jian et al. (1999). Paleo-climate simulation of 21 ka for Tibetan Plateau and eastern Asia. The 3rd PMIP Workshop, GEOTOP, University du Quebec a Montreal, Canada, October 4th to 8th, 1999.

Manabe, S. and Broccoli, A. J. (1985). The influence of continetal ice sheets on the climate of an ice age. *J. Geophys. Res.*, **90**: 2167—2190.

Martin, C., Kubatzki, C., Brovkin, V. et al. (1999). Simulation of an abrupt change in Sahara vegetation in the mid-Holocene. *Geophysical Research Letters*, **26**: 2037—2040.

McAvaney, B. J., Bourke, W. and Puri, K. (1978). A global spectral model for simulation of the general circulation. *Journal of Atmospheric Sciences*, **35**: 1557—1583.

Peltier, W. R. (1994). Ice age paleotopography. *Science*, **265**: 195—201.

Qin Boqiang and Yu Ge (1998). Implications of lake level fluctuations at 6 ka and 18 ka in mainland Asia. *Global and Planetary Change*, **18**: 59—72.

Rind, D. (1987). Components of ice age circulation. *J. Geophys. Res.*, **92**: 4241—4281.

Sellers, P. J., Mints, Y., Sud, Y. C. et al. (1986). A simple biosphere model (SiB) for use within general circulation models. *Journal of Atmospheric Sciences*, **43**: 505—531.

Shen Yongping and Xu Daoming (1994). Fluctuations of lakes and their environments since last glacial in Amdo Area, Tibet. *Journal of Glaciology and Geocryology*, **16**: 173—180.

Simmonds, I. (1985). Analysis of the "spinning" of a global circulation model. *Journal of Geophysical Research*, **90**: 5637—5660, .

Slingo, J. M. M., Blackburn, A., Betts, A. et al. (1994). Mean climate and transience in the tropics of UGAMP GCM: Sensitivity to convective parametrization. *Quarterly Journal of Royal Meteorology Society*. **120**: 881—922.

Street-Perrott, F. A., Marchand, D. S., Roberts, N. et al. (1989). Global lake-level variations from 18, 000 to 0 years ago: a palaeoclimatic analysis. Washington: U. S. DOE/ER/60304—H1 TR046. U. S. Department of Energy, Technical Report, 230.

Sun Jianghong and Ke Manhong (1995). Vegetation and climate of the Loess Plateau in China during the late Pleistocene. *Scientia Geologica Sinica*, Supplementary Issure, (**1**): 91—103.

Tarasov, P. E., Harrison, S. P., Saarse, L. et al. (1994). Lake status records from the former Soviet Union and Mongolia: Data base documentation. Boulder, NOAA Palaeoclimatology Publications Series Report 2, pp. 27.

Tarasov, P. E., Volkova, V. S., Webb, III T. et al. (1999). Last Glacial Maximum Biomes Reconstructed from Pollen and Plant Macrofossil Data from Northern Eurasia. *Journal of Biogeography* (submitted).

Valdes, P. J. and Hall, N. M. J. (1994). Mid-latitude depressions during the last ice-age. In *Long-Term Climate Variations—Data and Modeling*, Edited by J.-C. Duplessey and M. —T. Spyridakis, NATO ASI Series I. **22**: 510—532.

Wang Huijun (1999). Role of vegetation and soil in the Holocene megathermal climate over China. *Journal of Geophysical Research*, **104**: 9361—9367.

Wang Suming, Yu Yuansheng, Wu Ruijin et al. (1990). *Daihai Lake*. Hefei: China Science and Technolo'gy University Press, pp. 1—191 (in Chinese).

Winkler, M. G. and Wang, P. (1993). The late-quaternary vegetation and climate of China. In: Wright, H. E., Kutzbach, J. E., Webb, III T., et al. (Editors). *Global Climates Since the Last Glacial Maximum*, University of Minnesota Press, Minnesota, pp. 221—261.

Wright, Jr. H. E., Kutzbach, J. E., Webb, III. T. et al. (1993). *Global Climates Since the Last Glacial Maximum*, University of Minnesota Press, Minneapolis, pp. 468—513.

Wu Guoxiong, Liu Hui, Zhao Yucheng et al. (1996). A nine-layer atmospheric general circulation model and its performance. *Adv. Atmo. Sci.*, **13**: 1—17.

Xue Yongkang, Sellers, P. J., Kinter, J. L. et al. (1991). A simplified biosphere model for global climate studies. *Journal of Climate*, **4**: 345—364.

Yan Sun, Mu Guijin, Xu Yingqin et al. (1998). Quaternary environmental evolution of the Lop Nur region, China. *Acta Geographica Sinica*, **53**: 332—340 (in Chinese).

Yao Tangdong, Jiao Keqin and Zhang Xinping (1994). Climatic and environmental records from Guliya cap. *China Science* (D), **24**: 766—773.

Yu Ge and Harrison, S. P. (1995). Lake status records from Europe: Data base documentation. Boulder: NOAA Paleoclimatology Publications Series Report 3, pp. 451.

Yu Ge et al. (1999). Lake records and LGM climate in China. *Chinese Science Bulletin*, **45**: 1158—1164.